

The hippocampal formation participates in novel picture encoding: Evidence from functional magnetic resonance imaging

CHANTAL E. STERN*^{†‡}, SUZANNE CORKIN[§], R. GILBERTO GONZÁLEZ*[†], ALEXANDER R. GUIMARAES*[†], JOHN R. BAKER*[†], PEGGY J. JENNINGS[§], CINDY A. CARR*[†], ROBERT M. SUGIURA[§], VASANTH VEDANTHAM*[†], AND BRUCE R. ROSEN*[†]

*Massachusetts General Hospital–Nuclear Magnetic Resonance Center, Charlestown, MA, 02129; [†]Harvard Medical School, Boston, MA 02114; and [§]Department of Brain and Cognitive Sciences and the Clinical Research Center, Massachusetts Institute of Technology, Cambridge, MA 02139

Communicated by Emilio Bizzi, Massachusetts Institute of Technology, Cambridge, MA, May 13, 1996 (received for review December 5, 1995)

ABSTRACT Considerable evidence exists to support the hypothesis that the hippocampus and related medial temporal lobe structures are crucial for the encoding and storage of information in long-term memory. Few human imaging studies, however, have successfully shown signal intensity changes in these areas during encoding or retrieval. Using functional magnetic resonance imaging (fMRI), we studied normal human subjects while they performed a novel picture encoding task. High-speed echo-planar imaging techniques evaluated fMRI signal changes throughout the brain. During the encoding of novel pictures, statistically significant increases in fMRI signal were observed bilaterally in the posterior hippocampal formation and parahippocampal gyrus and in the lingual and fusiform gyri. To our knowledge, this experiment is the first fMRI study to show robust signal changes in the human hippocampal region. It also provides evidence that the encoding of novel, complex pictures depends upon an interaction between ventral cortical regions, specialized for object vision, and the hippocampal formation and parahippocampal gyrus, specialized for long-term memory.

The structures that are important for encoding and storage of novel information have been the focus of extensive research since the pioneering work of Scoville, Milner, and Penfield (1–4). A convergence of research in animals and humans has led to the hypothesis that the hippocampus and related medial temporal lobe structures are critical for the encoding of novel information for subsequent storage in the neocortex (2, 5–7). In humans, anterograde amnesia—the inability to learn new information—is associated with bilateral lesions of medial temporal lobe structures (2, 8). In nonhuman primates, single-unit recordings have identified neurons that respond preferentially to novel or familiar stimuli. These neurons are found in structures that receive output from the hippocampus [such as the anterior thalamus (9) and nucleus accumbens (10)] and in structures that provide afferent input to the hippocampus [such as the entorhinal cortex (11)]. Lesion studies in animals have provided extensive data on the role of medial temporal lobe structures in the performance of behavioral tasks requiring storage of novel information. For example, lesions of hippocampus and adjacent cortical structures, such as the perirhinal and entorhinal cortices, impair performance on delayed nonmatching to sample tasks in nonhuman primates (12) and rats (13). Controversies remain about the exact structures that are most important for the performance of explicit memory tasks (12–16).

Functional brain imaging studies have attempted to demonstrate the role of the hippocampus and related medial temporal lobe structures in the encoding and retrieval of long-term memories in the intact human brain. Several studies

using positron emission tomography have shown no evidence of a medial temporal lobe contribution to encoding and recognition (17–19); however, more recent reports have shown changes in the hippocampus in response to the encoding of objects and faces (20–23). The imaging studies that successfully demonstrated signal changes in the hippocampal formation differ from those that did not localize activity in the medial temporal lobe in the type of stimuli presented to the subject. Studies using verbal material have generally been unsuccessful (17–19, 24), whereas studies using object and face stimuli have shown medial temporal lobe changes (20–23).

The development of functional magnetic resonance imaging (fMRI) techniques (25, 26) provides a new tool for testing specific hypotheses about the anatomical and physiological substrates underlying the encoding of novel information in the human brain. In this study, we used a high-speed echo-planar scanning technique (27) to examine the encoding of complex, novel pictures in the intact human brain.

METHODS

Subjects. Eight healthy subjects (5 men, 3 women; age range, 19–43) participated in this study. Subjects were recruited from the Massachusetts Institute of Technology and Harvard University communities. All subjects gave informed consent in accordance with the Human Subjects Committee guidelines of the Massachusetts General Hospital.

Scanning Methods and Data Analysis. Conventional and echo-planar MR imaging were carried out using a high-speed scanner (1.5-T General Electric Signa scanner, modified by Advanced NMR Systems, Wilmington, MA). The subject was positioned in the scanner, and the head was immobilized using foam support cushions. Slice selection was determined by initially collecting a series of 59 sagittal, high-resolution, T1-weighted images through the brain. We positioned 7 mm-thick contiguous slices with 3 × 3 mm in-plane resolution coronally from the frontal pole to the occipital lobe. Coronal slices were chosen for this study to provide the maximum number of slices through the hippocampus and to avoid partial voluming effects, which would have been more prevalent had axial slices been chosen. In most subjects, 20 coronal slices allowed for complete brain coverage. After selecting the number and location of the slices, a series of high-resolution, T1-weighted images was taken for anatomically defining the high-speed functional images. An additional series of two-dimensional Spoiled Grass multiplanar T1-weighted flow-sensitive images were taken to locate large blood vessels running within the selected slices.

We used a receive-only radiofrequency quadrature head volume coil, which provided an average signal-to-noise ratio of

The publication costs of this article were defrayed in part by page charge payment. This article must therefore be hereby marked "advertisement" in accordance with 18 U.S.C. §1734 solely to indicate this fact.

Abbreviations: fMRI, functional magnetic resonance imaging; ROI, region-of-interest.

[‡]To whom reprint requests should be addressed.

$\approx 100:1$ in an individual image within the time series. An automatic shimming method further enhanced the signal-to-noise ratio and reduced the fMRI susceptibility artifacts present in the medial temporal lobe. An asymmetric spin-echo imaging sequence (28, 29), which is sensitive to signal changes arising from small changes in blood oxygenation levels, was used during fMRI scanning repetition time [(TR) = 2500, echo time (TE) = 50]. Preliminary set up and localizing scans required ≈ 30 min; the subsequent functional scans were acquired over an additional 60–90 min.

Task-induced changes in fMRI signal intensity were assessed using a nonparametric statistical analysis procedure that tests whether data acquired during an experimental task are likely to come from the same distribution as data acquired during control tasks (30). This analysis was performed in the following ten steps. (i) All slices and time points were reconstructed using unfiltered Fourier transforms from complete k-space data to form a volumetric time series magnitude image dataset. (ii) Each successive time point in the volumetric time series was registered to the first time point to compensate for any slow motion of the subject's head that occurred during a scan (31). (iii) Every magnitude image in the time series was spatially filtered using a two-dimensional Hamming window. The resulting voxel size was $6.25 \text{ mm} \times 6.25 \text{ mm} \times 7.0 \text{ mm}$ full-width at half-maximum. (iv) Each voxel location was treated independently to estimate the empirical cumulative distribution functions during the control (repeated picture) and experimental (novel picture) states. (v) The point(s) of maximal difference between the two estimated distribution functions—i.e., the Kolmogorov–Smirnov (KS) statistic, was computed for each voxel. (vi) The probability that this maximal difference could have occurred due to chance for each voxel was assembled into a volumetric probability map. (vii) The probability map was converted to a logarithmic color scale and was overlaid on anatomical images of the same location for visual inspection. (viii) The time course of activity within regions-of-interest (ROIs) that exhibited significant task-induced fMRI signal response, as determined by the KS probability map, were extracted from the volumetric time series magnitude image dataset and plotted. (ix) ROIs showing statistically significant differences between the control and experimental conditions were localized anatomically by visually inspecting the functional and high-resolution anatomical images for each subject. (x) Each individual scan was converted

into Talairach space, and the Talairach coordinates were computed for each ROI.

Task Design. A sequential task-activation paradigm was employed, alternating between an experimental condition for picture encoding and a control condition. During the experimental condition, subjects viewed 40 complex colored magazine pictures presented sequentially. Subjects were instructed to view the pictures carefully, so that they could recognize them later. The stimuli were projected using a video-computer hookup to a Sharp XG-2000f liquid crystal back-projection television monitor. The stimuli were displayed at a rate of one picture every 3 sec on a translucent screen placed ≈ 30 cm from the subjects' eyes. Subjects viewed the pictures through an overhead mirror. During the control condition, subjects viewed a single complex colored magazine picture, which was presented repeatedly at the same rate as the novel stimuli (every 3 sec). Scanning occurred over a 4-min block. Subjects performed the experimental task during the first and third minutes and the control task during the second and fourth. During each 4-min run, fMRI images were acquired throughout the brain every 2.5 sec.

Subjects subsequently performed a two-alternative forced choice recognition task to verify that they had encoded the 40 pictures. Each picture presented during the encoding task was paired with a novel picture. Subjects pressed a button to indicate which picture they had viewed previously.

RESULTS

In all subjects, the picture encoding task was associated with increased fMRI signal in the posterior portion of the hippocampus and adjacent parahippocampal gyrus. Fig. 1 shows the single subject results from a representative subject. A series of coronal, high-resolution T2 MR images of the brain are shown, with color regions indicating fMRI signal changes that reached statistical significance using the KS statistical test, superimposed on anatomical grayscale images. Localized fMRI signal was significantly elevated during the picture encoding task, relative to the control task.

Signal changes in the hippocampal region were highly consistent across all eight subjects at the $P < 0.001$ level. Activation was localized to include approximately the posterior quarter of the hippocampal formation and adjacent parahippocampal gyrus. Fig. 2 shows representative time courses

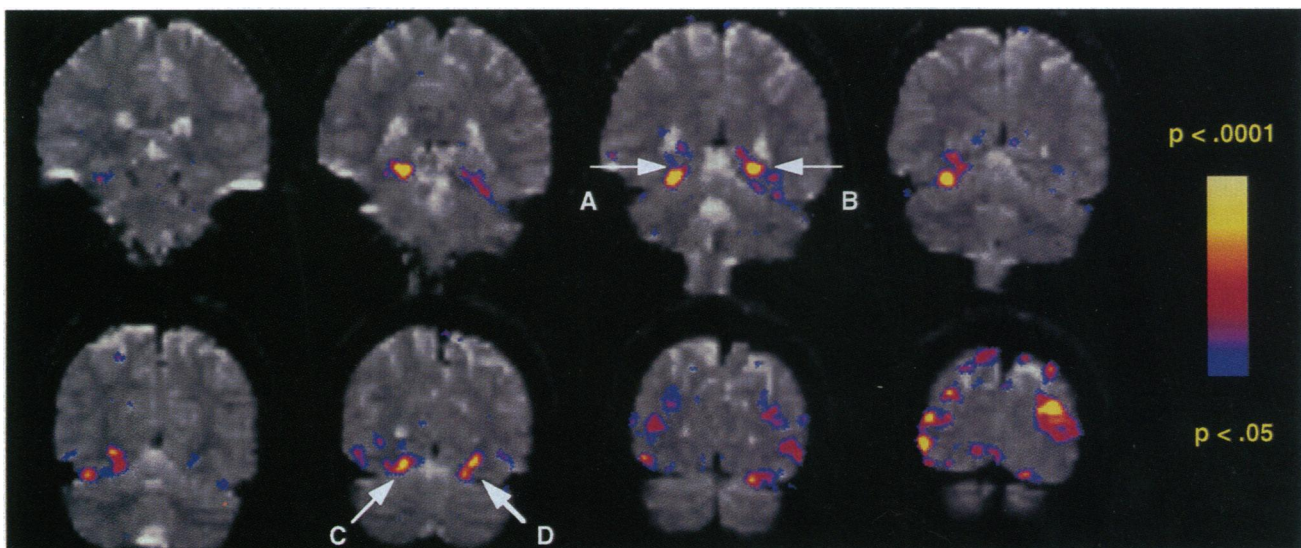


FIG. 1. A series of eight anatomical grayscale coronal images from anterior (Upper Left) to posterior (Lower Right) for a single subject. The left hemisphere appears on the right side of the figure, and the right hemisphere on the left. Areas with statistically significant fMRI signal intensity increases are shown superimposed in color, with blue representing a significance level of $P < 0.05$ and yellow a level of $P < 0.0001$. Arrows point to the posterior activation in the right (A) and left (B) hippocampal region and right (C) and left (D) lingual and fusiform gyri.

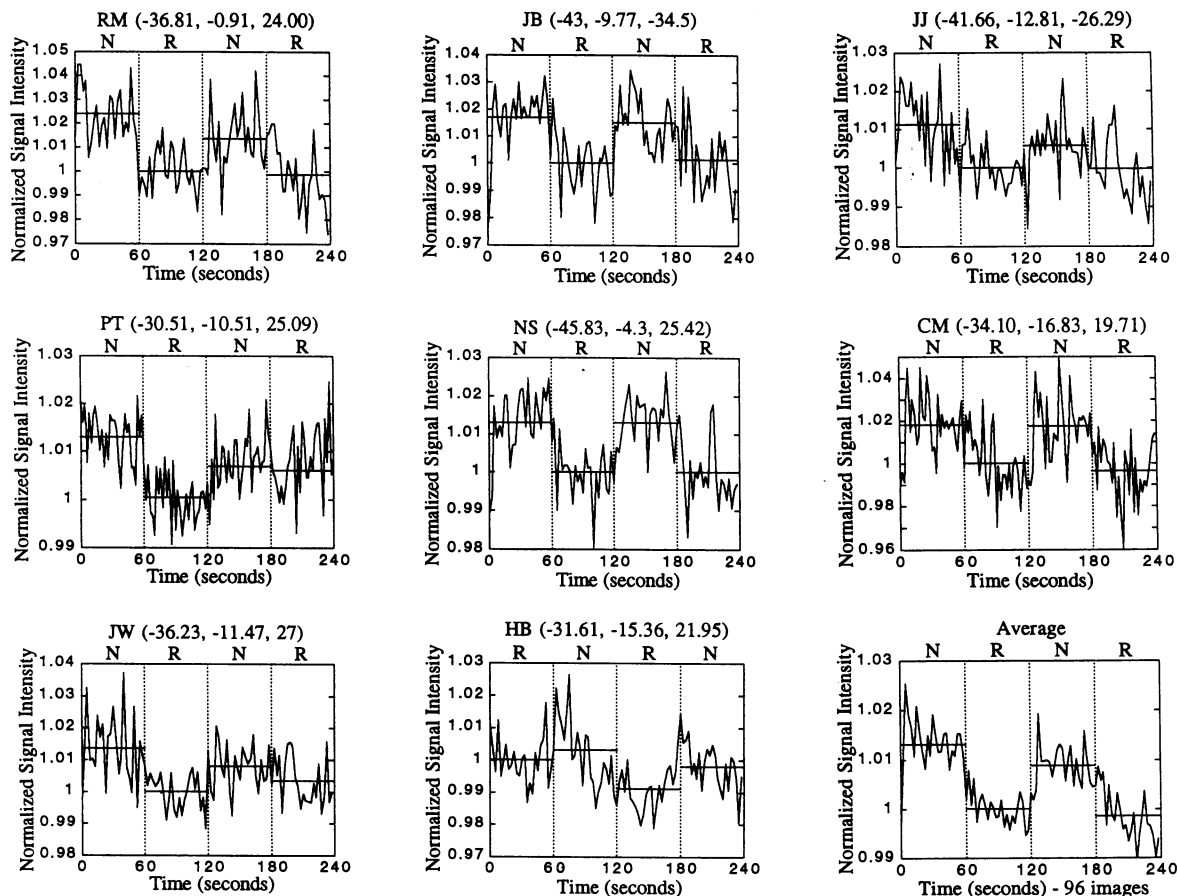


FIG. 2. Representative time courses from ROIs taken within the hippocampal region are shown for all eight subjects. The Talairach location of each ROI (posterior, inferior, and lateral) is given above each graph. The four time blocks represent the alternating 1-min novel (N) and repeating (R) conditions. Note that for subject HB, the order of the N and R conditions is reversed. Horizontal lines represent the average normalized signal intensity for each 1-min time block. Percentage signal changes for the individual subjects ranges between $\approx 1\%$ and 2.5% .

from the hippocampal region in all eight subjects, with the Talairach coordinates for the location of each ROI. All time courses were taken from ROIs containing more than four contiguous pixels. The percentage signal change between the two conditions for each individual subject ranged between $\approx 1\%$ and 2.5% (Fig. 2). The changes were bilateral in all subjects. From the averaged data (Fig. 3), it is evident that the signal changes occurring in the right hemisphere were greater than on the left. Additional bilateral signal changes at the $P < 0.001$ criterion were observed in the lingual and fusiform gyri in all subjects ($n = 6$) where these regions were studied. In the two remaining subjects, the size of the subject's head coupled with the limitation of the number of functional slices that could be collected resulted in the selection of fMRI slices that did not extend as far posteriorly as the lingual and fusiform gyri.

Significant fMRI signal intensity changes were not present in the anterior portion of the hippocampal formation, the amygdala, periamygdaloid cortex (area 51), perirhinal cortex (areas 35 and 36), and entorhinal cortex (area 28). No significant changes were noted in the frontal lobes during picture encoding. Fig. 3 presents the average functional data for all eight subjects superimposed on an average of all eight anatomical scans. The Talairach coordinates (lateral x , posterior y , and inferior z) of regions showing statistically significant changes in the averaged data are: left hippocampal region (x , -21.00 ; y , -31.87 ; and z , -7.50), left lingual and fusiform gyri (x , -21.00 ; y , -56.25 ; and z , -10.31), right hippocampal region (x , 28.00 ; y , -25.31 ; and z , -5.62), and right lingual and fusiform gyri (x , 35.00 ; y , -37.50 ; and z , -15.00).

The behavioral results of the subsequent picture recognition task demonstrated that subjects were able to identify previously viewed pictures at an accuracy rate ranging from 75% to 97% .

DISCUSSION

The results presented here provide evidence of activation-induced fMRI signal intensity changes in the human hippocampal formation. These results were highly consistent and indicate that fMRI can be used to study medial temporal lobe structures during such complex cognitive computations as the encoding and storage of novel stimuli. Our results contrast with some previous imaging studies that failed to elicit changes in medial temporal lobe structures during the acquisition and retrieval of verbal episodic information (19, 24). They concur, however, with recent positron emission tomography studies showing greater activity in the hippocampus during encoding of novel stimuli (32) and faces (20, 21). Additional studies have reported hippocampal activity during the recognition of possible but not impossible novel objects (22) and during the conscious recall of verbal stimuli that were encoded more effectively (high recall condition) than those that had not been encoded well (low recall condition) (23). Although further studies are necessary to elucidate the exact role of the hippocampus in recall and recognition, the results presented here suggest a role for the hippocampus in the encoding of complex visual information. Gaffan and Harrison (33) have suggested that damage to the hippocampal system disrupts a snapshot type of memory for the identity and spatial arrangement of objects within a visual scene. This "snapshot memory" could

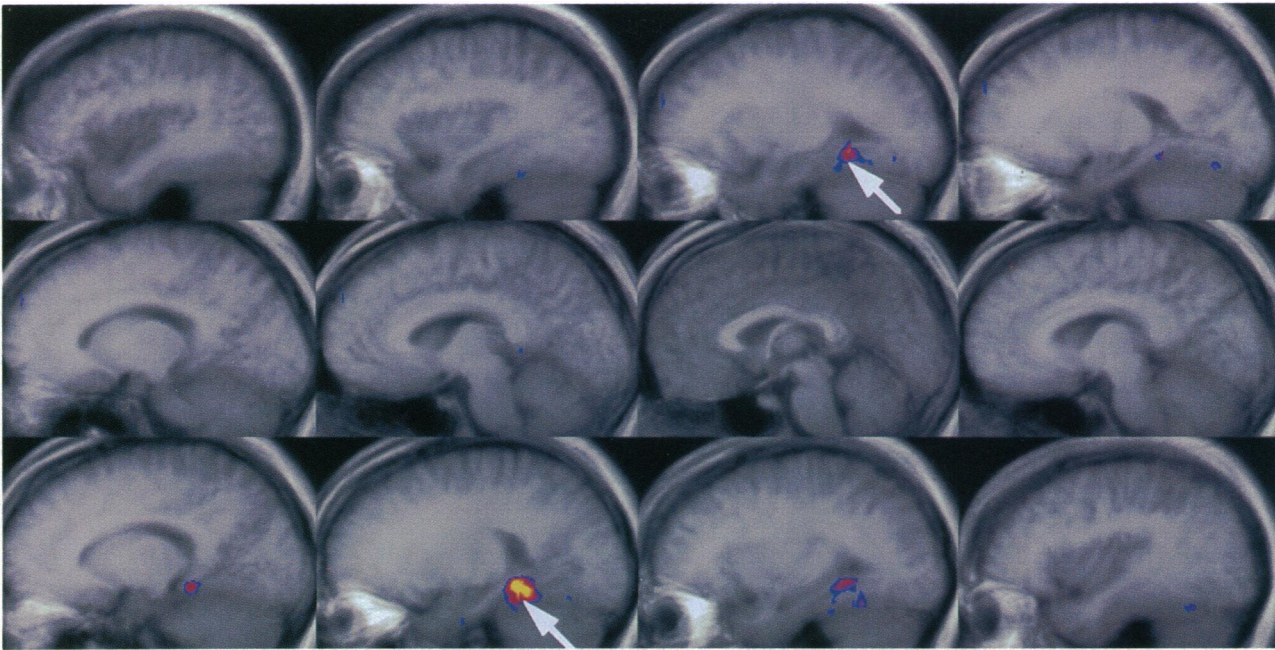


FIG. 3. Sagittal sections presenting the functional and anatomical data averaged across all eight subjects. The sequence of panels moves from left to right and top to bottom, with the upper left image representing the left lateral most section, and the bottom right image representing the right lateral most section. Midline sections are shown in the middle of row 2. Blue represents a significance level of $P < 0.05$, red a level of $P < 0.01$, and yellow a level of $P < 0.005$. The average Talairach coordinates (lateral, x ; posterior, y ; and inferior, z) are: left hippocampal region (-21.00 , -31.87 , and -7.50), left lingual and fusiform gyri (-21.00 , -56.25 , and -10.31), right hippocampal region (28.00 , -25.31 , and -5.62), right lingual and fusiform gyri (35.00 , -37.50 , and -15.00). Arrows indicate activity in the hippocampal and parahippocampal region. The upper arrow is shown in a section at a laterality of $x = 21$, and the lower arrow is shown in a section at a laterality of $x = 35$. Each section is 7 mm thick.

account for the hippocampal and parahippocampal activity found in this study and for the results of several other studies in which the visual and spatial characteristics of the information presented is important (20–22, 32). These imaging results, and the idea of the hippocampus performing a type of snapshot memory, are consistent with studies of temporal lobe lesions in man, which have shown deficits on object location tasks following right temporal lobectomy (34–36).

The localization of activation in the posterior hippocampal formation may relate to differences in the anatomical innervation of anterior versus posterior hippocampus (37). In single-unit recordings from nonhuman primates performing a delayed matching to sample task, several studies have noted more neurons that respond in the posterior as opposed to the anterior hippocampal formation (11, 38, 39). In another study of nonhuman primates, global ischemia produced selective damage to the hippocampus and dentate gyrus, with cell loss being greater in the posterior portion of the hippocampus than in the anterior portion. This limited posterior hippocampal damage was sufficient to impair delayed nonmatching to sample task performance (40). The localization of fMRI activity to the posterior hippocampal formation and parahippocampal gyrus supports the idea that these posterior hippocampal areas form an integrated system with a qualitatively different functional role from anterior subdivisions of the hippocampal system (7). The posterior hippocampal areas, however, are not sufficient to support normal memory function, as illustrated by the severely amnesic patient H.M., in whom the posterior 2 cm of the hippocampus and parahippocampal gyrus are preserved (Corkin *et al.*, unpublished results).

Another important finding was the absence of fMRI signal intensity changes in the amygdala, perirhinal cortex (areas 35 and 36), periamygdaloid cortex (area 51), and entorhinal cortex (area 28) during picture encoding. These findings address the debate regarding the role of the amygdala, perirhinal, and entorhinal cortices in the performance of memory tasks (6, 12, 15, 41, 42). Our findings are consistent with recent

human and animal studies showing that lesions confined to the hippocampal formation, but sparing the amygdala, entorhinal, and perirhinal cortices, are sufficient to cause memory impairments (40, 43). Previous imaging studies of encoding have reported significant changes in the dorsolateral prefrontal cortex during the acquisition of verbal episodic information (18, 19). We did not find changes in frontal cortex in this study. The lack of activity in the prefrontal cortex, together with the increases in medial temporal lobe activity cited here, suggests that visual and verbal material may be encoded using different pathways.

Additional signal intensity changes were noted in the fusiform and lingual gyri bilaterally. These signal changes underscore the importance of this region for visual object recognition. Damage to these areas in humans results in visual agnosia and prosopagnosia (44, 45), and these structures may correspond to the inferotemporal cortex in nonhuman primates, which has been shown to play a role in object discrimination and recognition (46–48). In recordings from the inferotemporal cortex in nonhuman primates, neurons show a stronger response to the initial presentation of a novel pattern than to subsequent presentations (11, 49–51). Responses of this type could underlie the greater activation found in lingual and fusiform gyri during presentation of novel pictures. In comparison, recordings of single-unit activity in the hippocampus indicate that hippocampal neurons respond on the basis of a match or mismatch of current input with previously stored information (52). This finding is consistent with theories suggesting that the hippocampus performs a comparison function that guides the formation of new representations (53–57). The activation changes found here may reflect the greater demand on this function of the hippocampus during sequential storage of novel pictures than during repeated contact with a familiar stimulus.

In addition to the object recognition components of encoding, there are attentional components. Novelty alone can result in heightened awareness of specific stimuli in a group of stimuli (“novel pop-out”; ref. 58), and attention to novelty plays an

integral role in encoding. In addition to encoding, these factors of novelty versus familiarity and attention may contribute to the increased fMRI signal noted in this study. In common with our study, activation in the parahippocampal, lingual, and fusiform gyri has been noted in a positron emission tomography study of selective attention to shape (59, 60). This similarity may reflect the fact that attention to and recognition of objects within a novel picture is a necessary component of the encoding and storage of that picture in memory. However, the Talairach locations of parahippocampal areas activated during attention to shape (59, 60) are anterior to the parahippocampal areas activated during novel picture encoding.

The hippocampal activation described here, along with recent positron emission tomography data showing activation of the hippocampus during encoding of objects (32) and faces (20, 21), contrasts with previous results (19, 24). We suggest that the lack of selective activation of the hippocampal region in previous studies and the activation of the hippocampal formation in recent studies is dependent upon the type and complexity of the information presented in the stimuli being encoded. Studies that have found localized changes in the hippocampus, including this one, have required that subjects view complex visual scenes or objects, including faces (20, 21, 32). These studies differ from studies of verbal material, which have generally not localized activity to the hippocampus (17, 19, 24). The key difference between imaging studies that do or do not show hippocampal activity is probably not specifically related to the use of verbal versus visual information, but more likely relates to the complexity and relational characteristics of the information being presented. Simple verbal stimuli, unlike complex visual pictures and faces, do not require the formation of new representations or relationships. These studies are consistent with the idea that the hippocampus performs a comparison function that guides the formation of new representations (53–56). The fMRI changes reported here suggest that the encoding of novel, complex pictures depends upon an interaction between hippocampal regions, specialized for long-term memory, and ventral cortical regions, specialized for object recognition.

We thank K. K. Kwong, R. M. Weisskoff, T. L. Davis, and J. W. Belliveau for development of the fMRI imaging technique and protocols; R. M. Weisskoff and T. L. Davis for statistical software; D. Kennedy and A. Jiang for motion correction software and Talairach transformation software; T. Reese for automatic shimming protocols; M. Snow for behavioral and eye movement detection programming; M. E. Hasselmo for comments on this manuscript; and J. H. Growdon and T. J. Brady for their valuable contributions to this study. We thank the staff and members of the Massachusetts General Hospital–Nuclear Magnetic Resonance Center and our subjects. This study was supported by the McDonnell–Pew Program in Cognitive Neuroscience Grant 92-39 and by the National Institutes of Health Grants AG10679, AG06605, AG05134, and AG05571.

1. Scoville, W. B. (1954) *J. Neurosurg.* **11**, 64–66.
2. Scoville, W. B. & Milner, B. (1957) *J. Neurol. Neurosurg. Psychiatr.* **20**, 11–21.
3. Penfield, W. & Milner, B. (1958) *Arch. Neurol. Psychiatr.* **79**, 475–497.
4. Milner, B. & Penfield, W. (1955) *Trans. Am. Neurol. Assoc.* **80**, 42–48.
5. Squire, L. R. & Zola-Morgan, S. (1991) *Science* **253**, 1380–1386.
6. Squire, L. R. (1992) *Psych. Rev.* **99**, 195–231.
7. Eichenbaum, H., Otto, T. & Cohen, N. (1992) *Behav. Neural Biol.* **57**, 2–36.
8. Corkin, S. (1984) *Semin. Neurol.* **4**, 249–259.
9. Rolls, E. T., Perrett, D. I., Cann, A. W. & Wilson, F. A. W. (1982) *Brain* **105**, 611–646.
10. Williams, G. V., Rolls, E. T., Leonard, C. M. & Stern, C. E. (1993) *Behav. Brain Res.* **55**, 243–252.
11. Riches, I. P., Wilson, F. A. W. & Brown, M. W. (1991) *J. Neurosci.* **11**, 1763–1779.

12. Zola-Morgan, S., Squire, S., Amaral, D. G. & Suzuki, W. A. (1989) *J. Neurosci.* **9**, 4355–4370.
13. Otto, T. & Eichenbaum, H. (1992) *Behav. Neurosci.* **106**, 762–775.
14. Squire, L. R., Zola-Morgan, S. & Chen, K. (1988) *Behav. Neurosci.* **11**, 210–221.
15. Mishkin, M. (1978) *Nature (London)* **273**, 297–298.
16. Horel, J. A. (1978) *Brain* **101**, 403–445.
17. Buckner, R. L., Petersen, SEM, Ojemann, J. G., Miezin, F. M., Squire, L. R. & Raichle, M. E. (1995) *J. Neurosci.* **15**, 12–29.
18. Squire, L. R., Ojemann, J. G., Miezin, F. M., Petersen, S. E., Videen, T. O. & Raichle, M. E. (1992) *Proc. Natl. Acad. Sci. USA* **89**, 1837–1841.
19. Shallice, T., Fletcher, P., Frith, C. D., Grasby, P., Frackowiak, R. S. J. & Dolan, R. J. (1994) *Nature (London)* **368**, 633–635.
20. Grady, C. L., McIntosh, A. R., Horowitz, B., Maisog, J. M., Ungerleider, L. G., Mentis, M. J., Pietrini, P., Schapiro, M. B. & Haxby, J. V. (1995) *Science* **269**, 218–220.
21. Haxby, J. V., Ungerleider, L. G., Horowitz, B., Maisog, J. M., Rapoport, S. I. & Grady, C. L. (1995) *Proc. Natl. Acad. Sci. USA* **93**, in press.
22. Schacter, D. L., Reiman, E., Uecker, A., Polster, M. R., Yun, L. S. & Cooper, L. A. (1995) *Nature (London)* **376**, 587–590.
23. Schacter, D. L., Alpert, N. M., Savage, C. R., Rauch, S. L. & Albert, M. S. (1996) *Proc. Natl. Acad. Sci. USA* **93**, 321–325.
24. Grasby, P. M., Frith, C. D., Friston, K. J., Bench, C., Frackowiak, R. S. J. & Dolan, R. J. (1993) *Brain* **116**, 1–20.
25. Kwong, K. K., Belliveau, J. W., Chesler, D. A., Goldberg, I. E., Weisskoff, R. M., Poncelet, B. P., Kennedy, D. N., Hoppel, B. E., Cohen, M., Turner, R., Cheng, H., Brady, T. & Rosen, B. R. (1992) *Proc. Natl. Acad. Sci. USA* **89**, 5675–5679.
26. Ogawa, S., Tank, D. W., Menon, R., Ellermann, J. M., Kim, S. G., Merkle, H. & Ugurbil, K. (1992) *Proc. Natl. Acad. Sci. USA* **89**, 5951–5955.
27. Mansfield, P. (1977) *J. Phys. C* **10**, L55–L58.
28. Dixon, W. T. (1984) *Radiology* **153**, 189–194.
29. Sepponen, R. E., Sepponen, J. T. & Tanttu, J. I. (1984) *J. Comput. Assist. Tomogr.* **8**, 585–587.
30. Stuart, A. & Ord, J. K. (1991) *Kendall's Advanced Theory of Statistics* (Oxford Univ. Press, New York).
31. Jiang, A., Kennedy, D. N., Baker, J. R., Weisskoff, R. M., Tootell, R. B. H., Woods, R. P., Benson, R. R., Kwong, K. K., Belliveau, J. W., Brady, T. J., Rosen, B. R. & Belliveau, J. W. (1995) *Human Brain Map* **3**, 224–235.
32. Tulving, E., Markowitsch, H. J., Kapur, S., Habib, R. & Houle, S. (1994) *NeuroReport* **5**, 2525–2528.
33. Gaffan, D. & Harrison, S. (1989) *Exp. Brain Res.* **74**, 202–212.
34. Pigott, S. & Milner, B. (1993) *Neuropsychologia* **31**, 1–15.
35. Smith, M. L. & Milner, B. (1981) *Neuropsychologia* **19**, 781–793.
36. Smith, M. L. & Milner, B. (1989) *Neuropsychologia* **27**, 71–81.
37. Amaral, D. G. & Witter, M. P. (1989) *Neuroscience* **31**, 571–591.
38. Watanabe, T. & Niki, H. (1985) *Brain Res.* **325**, 241–254.
39. Colombo, M. & Gross, C. G. (1994) *Behav. Neurosci.* **108**, 443–455.
40. Zola-Morgan, S., Squire, L. R., Rempel, N. L. & Clower, R. P. (1992) *J. Neurosci.* **12**, 2582–2596.
41. Murray, E. A. (1990) *Neurobiology of Comparative Cognition*, eds. Kesner, R. & Olton, D. (Erlbaum, Hillsdale, NJ).
42. Zola-Morgan, S., Squire, L. R. & Amaral, D. G. (1989) *J. Neurosci.* **9**, 1922–1936.
43. Zola-Morgan, S., Squire, L. R. & Amaral, D. G. (1986) *J. Neurosci.* **6**, 2950–2967.
44. Meadows, J. C. (1974) *Brain* **97**, 615–632.
45. Damasio, A. R., Tranel, D. & Damasio, H. (1990) *Annu. Rev. Neurosci.* **13**, 89–109.
46. Iwai, E. & Mishkin, M. (1969) *Exp. Neurol.* **25**, 585–595.
47. Mishkin, M., Ungerleider, L. G. & Macko, K. A. (1983) *Trends Neurosci.* **6**, 414–417.
48. Ungerleider, L. G. & Mishkin, M. (1982) in *Analysis of Visual Behavior*, eds. Ingle, D., Goodale, M. & Mansfield, R. (Massachusetts Institute of Technology Press, Cambridge, MA), 549–580.
49. Baylis, G. C. & Rolls, E. T. (1987) *Exp. Brain Res.* **65**, 614–622.
50. Rolls, E. T., Baylis, G. C., Hasselmo, M. E. & Nalwa, V. (1989) *Exp. Brain Res.* **76**, 153–164.
51. Miller, E. K., Li, L. & Desimone, R. (1991) *Science* **254**, 1377–1379.

52. Otto, T. & Eichenbaum, H. (1992) *Hippocampus* **2**, 323–334.
53. Gray, J. A. (1982) *The Neuropsychology of Anxiety: An Enquiry into the Functions of the Septo-Hippocampal System* (Oxford Univ. Press, New York).
54. Carpenter, G. A. & Grossberg, S. (1993) *Trends Neurosci.* **16**, 131–137.
55. Eichenbaum, H. & Buckingham, J. (1990) in *Learning and Computational Neuroscience: Foundation of Adaptive Networks*, eds. Gabriel, M. & Moore, J. (Massachusetts Institute of Technology Press, Cambridge, MA), pp. 171–231.
56. Hasselmo, M. E. & Schnell, E. (1994) *J. Neurosci.* **14**, 3898–3914.
57. Levy, W. B. (1989) in *Computational Models of Learning in Simple Neural Systems*, eds. Hawkins, R. D. & Bower, G. H. (Academic, Orlando, FL), pp. 243–305.
58. Johnston, W. A., Hawley, K. J. & Farnham, J. M. (1993) *J. Exp. Psych.* **19**, 140–153.
59. Corbetta, M., Miezin, F. M., Dobmeyer, S., Shulman, G. L. & Petersen, S. E. (1990) *Science* **248**, 1556–1559.
60. Corbetta, M., Miezin, F. M., Dobmeyer, S., Shulman, G. L. & Petersen, S. E. (1991) *J. Neurosci.* **11**, 2383–2402.